

**Forschungszentrum Karlsruhe**

Technik und Umwelt

Wissenschaftliche Berichte

FZKA 6652

**Actinide Migration Experiment in the  
HRL ÄSPÖ, Sweden: Results of Laboratory and  
In Situ Experiments (Part I)**

P. Vejmelka, B. Kienzler, J. Römer, Ch. Marquardt,  
E. Soballa, F. Geyer, T. Kisely, D. Heathman

Institut für Nukleare Entsorgung  
Hauptabteilung Informations- und Kommunikationstechnik

Forschungszentrum Karlsruhe GmbH, Karlsruhe

2001

**Impressum der Print-Ausgabe:**

**Als Manuskript gedruckt  
Für diesen Bericht behalten wir uns alle Rechte vor**

**Forschungszentrum Karlsruhe GmbH  
Postfach 3640, 76021 Karlsruhe**

**Mitglied der Hermann von Helmholtz-Gemeinschaft  
Deutscher Forschungszentren (HGF)**

**ISSN 0947-8620**

## **Acknowledgement**

The work was performed within the Project Agreement for collaboration on certain experiments related to the disposal of radioactive waste in the Hard Rock Laboratory Äspö (HRL) between the Bundesministerium für Wirtschaft (BMWi) and Svensk Kärnbränslehantering AB (SKB).

The authors thank the staff of HRL for preparation of rock and water samples, for the excellent cooperation and the maintenance of the proper operation of our glovebox.

# Actinide Migration Experiment in the HRL ÄSPÖ, Sweden: Results of Laboratory and In Situ Experiments (Part I)

## Abstract

Within the scope of a bilateral cooperation an **Actinide Migration Experiment** is performed by INE at the Äspö Hard Rock Laboratory in Sweden. This report covers investigations on actinide migration in single fractured granite samples (cores) performed in laboratory and in situ in the Äspö HRL. For the in situ experiment the CHEMLAB-2 probe developed by SKB and KTH, Stockholm is applied. Design of experimental setup, breakthrough of inert tracer and of the actinides Am, Np and Pu are presented. Breakthrough curves are analyzed to determine hydraulic properties of the fractured samples. Destructive and non-destructive analyses of the samples are performed. The different analytical techniques for characterization of the flow path and the sorbed actinides are presented. After cutting of the samples the abraded material is analyzed, the slices are used to visualize the flow path. Effective volumes and inner surface areas are measured. It is found that the fractured granite samples investigated show different characteristics. One-dimensional transport model calculation are performed and the results are compared to the experimental findings. The rather simple model is not well suited for the complex flow paths and the complicated sorption processes. Matrix diffusion processes are not relevant for cores investigated. It is shown that the CO<sub>2</sub> partial pressure of laboratory test and under in situ conditions results in the same speciation of the actinide elements under consideration. In the experiments only a breakthrough of Np(V) is observed. The recovery of Np(V) is in any case  $\leq 40\%$ . Recovery of Am(III) and Pu(IV) as well as of Np(IV) is not detected.

# **Actiniden Migration Experiment im Untertagelabor ÄSPÖ, Schweden: Ergebnisse von Labor und In Situ Experimenten (Teil I)**

## **Zusammenfassung**

Im Rahmen einer bilateralen Zusammenarbeit wurde vom INE ein erstes Actiniden-Migrations-Experiment im Hard Rock Laboratory Äspö in Schweden durchgeführt. Dieser Bericht beinhaltet Untersuchungen zur Actinidenmigration in einfach geklüfteten Granitproben, die im Labor und unter in situ Bedingungen im Untertagelabor Äspö durchgeführt wurden. Für die in situ Versuche wurde die CHEMLAB-2 Sonde verwendet, die von SKB und der KTH, Stockholm entwickelt wurde. Die Auslegung der Experimente, der Durchbruch von inerten Tracer und der Actiniden Am, Np und Pu werden vorgestellt. Die Durchbruchskurven werden hinsichtlich der hydraulischen Eigenschaften der geklüfteten Probe ausgewertet. Es werden zerstörungsfreie und zerstörende analytische Techniken an den Proben eingesetzt. Diese erlauben den Fließweg und die sorbierten Actiniden zu erfassen. Nach dem Zerschneiden der Proben wird das abgeschliffene Material analysiert, die Schnitte werden bezüglich des Fließwege visualisiert. Die effektiven Volumina der Kluff und ihren inneren Oberflächen werden vermessen. Die untersuchten Granitbohrkerne zeigen unterschiedliche Charakteristika. Rechnungen werden mit einem eindimensionalen Transportcode durchgeführt. Dieses Modell ist jedoch nicht hinreichend um die komplexen Fließwege und die komplizierten Sorptionsprozesse zu beschreiben. Matrix-Diffusionsprozesse spielen bei den hier untersuchten Proben keine wesentliche Rolle. Es wird gezeigt, dass unter den CO<sub>2</sub> Partialdrücken im Labor und unter in situ Bedingungen sich die Speziation der Actiniden nicht verändert. In den Experimenten wird ein Durchbruch nur für Np(V) beobachtet. Der gemessene Wiedererhalt liegt immer  $\leq 40\%$ . Am(III) und Pu(IV) sowie Np(IV) konnten in den eluierten Lösungen nicht nachgewiesen werden.

## Content

Abstract	i
Zusammenfassung	ii
Content	iii
List of Tables	iv
List of Figures	iv
1 Background	1
2 Objectives	1
3 Experimental concept	1
4 Results	3
4.1 Laboratory migration experiments	3
4.2 In situ migration experiment	5
4.3 Flow path analyses	6
4.3.1 Nondestructive method	7
4.3.2 Destructive method	8
4.4 Actinides sorbed onto inner surfaces of fractures	11
5 Interpretation of results and discussion	13
5.1 Hydraulic properties	16
5.2 Actinide speciation	17
5.3 Modeling actinide breakthrough and recovery	20
5.4 Matrix diffusion?	22
6 Summary and conclusions	23
7 References	24

## List of Tables

Tab. I	Characteristic data of the prepared cores (laboratory)	3
Tab. II	Overview about the experiments performed with core #1	4
Tab. III	Evaluation of fracture geometry from slices cut from core #1	10
Tab. IV	Mass and surface related Rs values of Am onto granitic material	14
Tab. V	Hydraulic properties of core #2	17
Tab. VI	Composition of groundwater from CHEMLAB-2 drill hole	18

## List of Figures

Fig. 1	Äspö core samples embedded in a stainless steel sleeve; top and bottom ends.	2
Fig. 2	Breakthrough curve for $^{237}\text{Np}$ determined for core #4 at INE laboratory.	4
Fig. 3	INE glovebox installed in a container close to the CHEMLAB II drillhole	5
Fig. 4	Breakthrough curves for tritiated water and for the total $\alpha$ -concentration from the first in situ CHEMLAB actinide migration experiment.	6
Fig. 5	X-ray computer tomography of core #3	7
Fig. 6	Scans of slice #7 (left) and #11 (right) of core sample #1	8
Fig. 7	Scan of slice #1, #10 (top) and #20 and #31 (bottom) of core #2 (used in the first in situ experiment).	9
Fig. 8	Distribution of volume and inner surfaces of the fracture along core #1	10
Fig. 9	3-D visualization of the fracture in core #1 by means of AVS software	11
Fig. 10	Distributions of $^{237}\text{Np}$ and $^{243}\text{Am}$ along the fracture of core #1 by analysis of the material abraded during the cutting of slices.	12
Fig. 11	Investigations of distribution of actinides across a slice of core #1, preliminary results.	12
Fig. 12	Locally sorbed actinide surface density (Np and Am) determined in core #1	13
Fig. 13	Locally sorbed $^{243}\text{Am}$ distribution in core #1	15
Fig. 14	Speciation of plutonium in Äspö groundwater in dependence on the $\text{CO}_2$ partial pressure.	18
Fig. 15	Speciation of neptunium in Äspö groundwater in dependence on the $\text{CO}_2$ partial pressure.	19
Fig. 16	Speciation of americium in Äspö groundwater in dependence on the $\text{CO}_2$ partial pressure.	19
Fig. 17	UV-VIS-NIR spectroscopy of eluted solution sampled in the breakthrough peak of the CHEMLAB experiment (core #2) at Äspö HRL.	20
Fig. 18	Comparison between computed and experimental breakthrough for the CHEMLAB experiment (core #2)	21
Fig. 19	Breakthrough curves obtained in core #2 for HTO pulse injection.	22

# Actinide Migration Experiment in the HRL ÄSPÖ, Sweden Results of Laboratory and In Situ Experiments (Part I)

## 1 Background

Groundwater flow through fractures in granitic host rocks may cause migration of actinides from the repository. In order to evaluate the impact of the migration processes on the release of radioactivity, complexation, sorption and colloid formation of actinides in the presence of the rock and weathered materials have to be investigated. Actinide elements show a very complex geochemical behavior which is influenced by changes of redox states of the elements, complexation with groundwater constituents and colloid formation. Sorption of actinides depends strongly on the actual speciation in the groundwater. Investigation of sorption behavior under the most realistic conditions attainable is required. Within the scope of a bilateral cooperation between SKB and FZK-INE, *Actinide Migration Experiments* are continuously conducted at the Äspö Hard Rock Laboratory. To guarantee most realistic conditions, the experiments are designed to fit into the CHEMLAB II probe.

## 2 Objectives

The Äspö Hard Rock Laboratory (HRL) was established in Sweden in a granite rock formation for in situ experiments with radionuclides (Backblom 1991). Within the scope of a bilateral cooperation, migration experiments with actinides such as Pu, Am, and Np were planned, designed and are performed by FZK-INE. These experiments aim to study sorption and migration behavior of these elements under the most realistic conditions attainable. A previous report summarizes laboratory sorption experiments as well as modeling and the design of the in situ experiments (Vejmelka 2000).

The objectives of the experiments are:

- to investigate the applicability of radionuclide retention coefficients measured in laboratory batch experiments for in situ conditions
- to validate the radionuclide retardation measured in laboratory in in situ experiments in rock
- to demonstrate that the laboratory data are reliable and correct under the conditions prevailing in the natural rock
- to reduce the uncertainty in the retardation properties and the governing processes for the radionuclides americium, neptunium and plutonium.

## 3 Experimental concept

In a first step, the experimental setup was designed and some preliminary sorption experiments with fracture filling material and granite, respectively, and with groundwater from the area of CHEMLAB II (Jansson 1997) were conducted in the laboratory at INE. To run the migration experiments in CHEMLAB II, a drill core sample with a fracture is placed into an autoclave. Core samples with a continuous fracture are chosen and placed in a sleeve of stainless steel. The periphery is filled with epoxy resin. The top and the bottom ends are



closed with acrylic glass covers sealed relative to the stainless steel sleeve with an O-ring. The lids are equipped with bores for feeding and extracting the groundwater lines. Remaining space between the lid and the granite cores is minimized by application of specifically prepared plastic seals.

Fig. 1 shows core samples with the fractures situated in open autoclaves.



Fig. 1 Äspö core samples embedded in a stainless steel sleeve; top and bottom ends.

The tightness of the autoclaves is tested in laboratory experiments, indicating leak-tightness up to 60 bar of groundwater pressure. The fluid pressure in CHEMLAB II is about 27 bar; consequently, no leakage of the columns is to be expected under in situ conditions. A total of four autoclaves of appropriate dimensions are prepared from the core samples available. Properties of the cores are listed in Tab. I.

In order to evaluate actinide breakthrough through the fractured rock samples and actinide recovery as a function of the eluted groundwater volume, the hydraulic properties of fractured rock samples are investigated at INE. HTO is used as inert tracer; dependencies of the breakthrough from the applied flow rates are recorded.

At Äspö HRL an inert gas glovebox is installed close to the CHEMLAB II drillhole. Tubing from the core in the CHEMLAB probe ends in the glovebox. The box contains a sample collector and a balance for recording the breakthrough as well as equipment required for groundwater sample preparations.

Based on geochemical model calculations actinide tracer cocktails are prepared according to the maximum solubilities of the actinides in the specific groundwater. The isotopes  $^{244}\text{Pu}$ ,  $^{243}\text{Am}$ , and  $^{237}\text{Np}$  are chosen due to their long half-lives and low specific radioactivity. Cocktails are prepared using groundwater from Äspö HRL (Tab. VI). Long-lived actinide concentrations in the "ÄSPÖ cocktail" were prepared as follows:

Pu-244	approx. $1 \times 10^{-8}$ mol/l
Am-243	approx. $1 \times 10^{-6}$ mol/l in laboratory, $1 \times 10^{-8}$ mol/l at Äspö
Np-237	approx. $1 \times 10^{-5}$ mol/l

Total  $\alpha$ -activity of the cocktail amounts to  $1.8 \times 10^4$  Bq/l.

Up to now, four core samples are prepared and tested in laboratory. The characteristics are given in Tab. I. Some more samples are under preparation, at present.

Tab. I Characteristic data of the prepared cores (laboratory)

	<b>Core 1</b>	<b>Core 2</b>	<b>Core 3</b>	<b>Core 4</b>
<b>Flow rate [ml/min]</b>	> 0.05	0.05 / 0.001	0.05	0.01
<b>Length [cm]</b>	10.5	15.0	18.0	15.0
<b>Pore Volume [ml]</b>	~ 0.7	~ 1.0	~1.0	~1.0
<b>Pressure drop [bar]</b>	-	12 / 3	23	44
<b>Remarks</b>	Test core	to be used in CHEMLAB	redundancy for CHEMLAB	actinide experiments in laboratory

## 4 Results

### 4.1 Laboratory migration experiments

One autoclave with embedded drill core is used in laboratory actinide migration tests applying the same conditions as expected in the Äspö HRL. The effective pore volume of the fracture in the drill core is measured to be 1 ml.

By use of a calibrated sample loop, the actinide cocktail with pH 7 is injected. The flow rate is chosen to be 0.3 ml/h (7.2 ml/day). Eluted groundwater is collected in samples of 1.5 ml. These samples are filtrated (450 nm) and analyzed by liquid scintillation counting (LSC). By means of  $\alpha$ -spectroscopy  $^{237}\text{Np}$  and  $^{243}\text{Am}$  are distinguished. Total  $^{243}\text{Am}$  concentration of eluted water is  $1 \times 10^{-11}$  mol/l. Recovery of Np is determined to be 26% of the injected quantity. The breakthrough curve is determined by the mass of the groundwater samples and the measured activity concentrations. The eluted groundwater volume in this experiment amounts to 60 to 80 ml.

Tab. II Overview about the experiments performed with core #1

Test #	Pulse μl	flow rate ml/min	Eluted volume ml	velocity mm/min	Time min
1	100	0.05	17	0.996	340
2	50	0.05	10	0.996	200
3	50	0.05	20	0.996	400
4	50	0.05	10	0.996	200
5	50	0.05	10	0.996	200
6	50	0.05	10	0.996	200
7	50	0.05	30	0.996	600
8	50	0.001	25	0.020	25000
9	50	0.001	40	0.020	40000

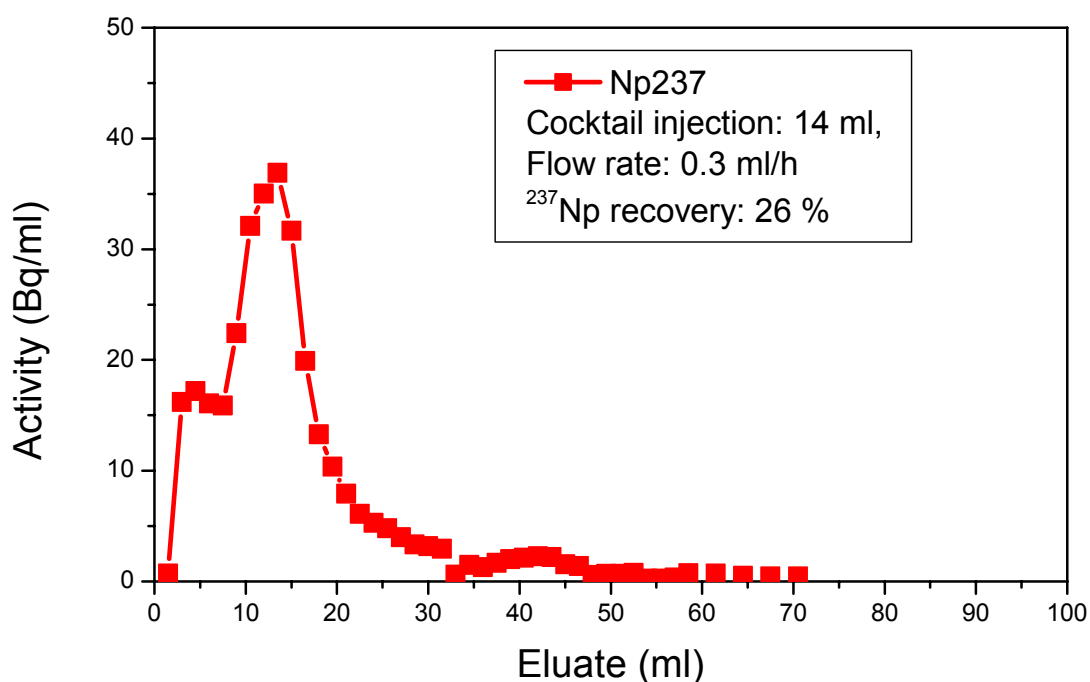


Fig. 2 Breakthrough curve for <sup>237</sup>Np determined for core #4 at INE laboratory.

The eluted water has the same pH as the injected water, Eh is measured to be +20 mV. However, in some experiments measured Eh was in the range of -200 mV. This finding is related to the limited redox buffer capacity of the groundwater.

Additional experiments showed significantly lower Np concentration in the effluent. These results support our hypothesis that Np(V) will be reduced to Np(IV) on the inner surfaces of the rock sample and subsequently be sorbed.

## 4.2 In situ migration experiment

After installation of the glovebox, test runs were performed. The first in situ actinide migration experiment was started at Äspö in October 2000. A 100 ml reservoir containing the actinide-groundwater cocktail was inserted into the CHEMLAB II probe. Additionally to the actinides, the cocktail was spiked by HTO. The HTO tracer was introduced for online controlling of the experiment. CHEMLAB II was equipped with the drill core in the autoclave and the reservoir at BASELAB laboratory. It was put in place, coupled to the glove box and a test run was performed for 5 days. After successful operation, a volume of 15 ml of actinide cocktail from the reservoir was injected into the fractured rock sample at a flow rate of 0.3 ml/h. Injection of this volume required 50 hours, afterwards natural groundwater was pumped for another 5 days at constant flowrate. After this period, it was intended to increase the flowrate. However, a technical defect of the CHEMLAB II probe interrupted the experiment. The eluted groundwater samples were transferred to INE. Fig. 4 shows the breakthrough curves for HTO and for the total  $\alpha$ -activity of the in situ experiment.



Fig. 3 INE glovebox installed in a container close to the CHEMLAB II drillhole  
The image shows the large main antechamber and the control unit and on the right side the CHEMLAB II drill hole lock

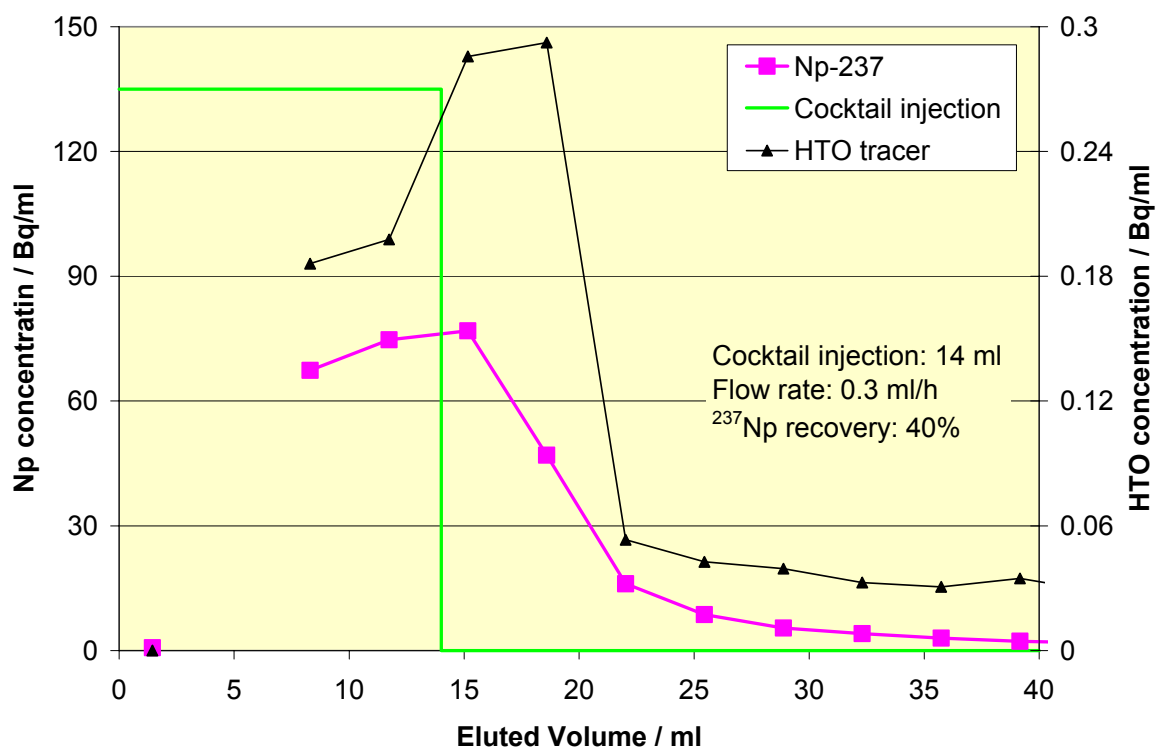


Fig. 4 Breakthrough curves for tritiated water and for the total  $\alpha$ -concentration from the first in situ CHEMLAB actinide migration experiment.

x axis corrected with respect to 30% loss of water by evaporation during sampling period.

The measured pH in the eluted samples was pH 7, Eh ranged from +30 to -60 mV. Fig. 4 shows measured activity in the eluted samples after filtration by 450 nm filters. ICP-MS measurements resulted in  $^{243}\text{Am}$  and  $^{244}\text{Pu}$  the concentrations below the detection limit of  $1 \times 10^{-12}$  mol/l. Based on these findings one can conclude that only  $^{237}\text{Np}$  contributes to the measured  $\alpha$ -concentration in the effluent. This result is equivalent to the results obtained by the first migration experiment in the laboratory. The recovery of  $^{237}\text{Np}$  is computed to be 40% of the injected quantity.

### 4.3 Flow path analyses

The cores used in these experiments were analyzed with respect to the flow path and to the interactions between dissolved actinides and the solid phases. Analysis of the flow path is performed by different methods: destructive and nondestructive investigations, such as X-ray computer tomography.

### 4.3.1 Nondestructive method

At first, the geometry of the flow path along the fractures was investigated by means of nondestructive X-ray computer tomography<sup>a</sup>. The method was applied to core #3. As radiation source a 420 kV X-ray tube, having a focus diameter of 1.5 mm was applied. Measurements were performed by 15 detectors at collimator sizes of 0.8x1.5 mm. Evaluated volume elements of the core had a volume of 0.2x0.2x1.5 mm<sup>3</sup>. However, resolution was not sufficient to reveal a continuously developed flow path. The aperture for the fracture in the core #3 was too narrow to be quantified by this method. An overview of the results is shown in Fig. 5. Dark areas indicate lower densities. The steel mantle can be seen clearly, also using a high-resolution monitor some structures are detectable, such as the epoxy resin between steel autoclave and granitic material. In the inner regions of the core, some small structures can be found. However the color of these structures are more light-colored, indicating higher density. This can be explained by a different material composition in these structures, but not by an open fracture.

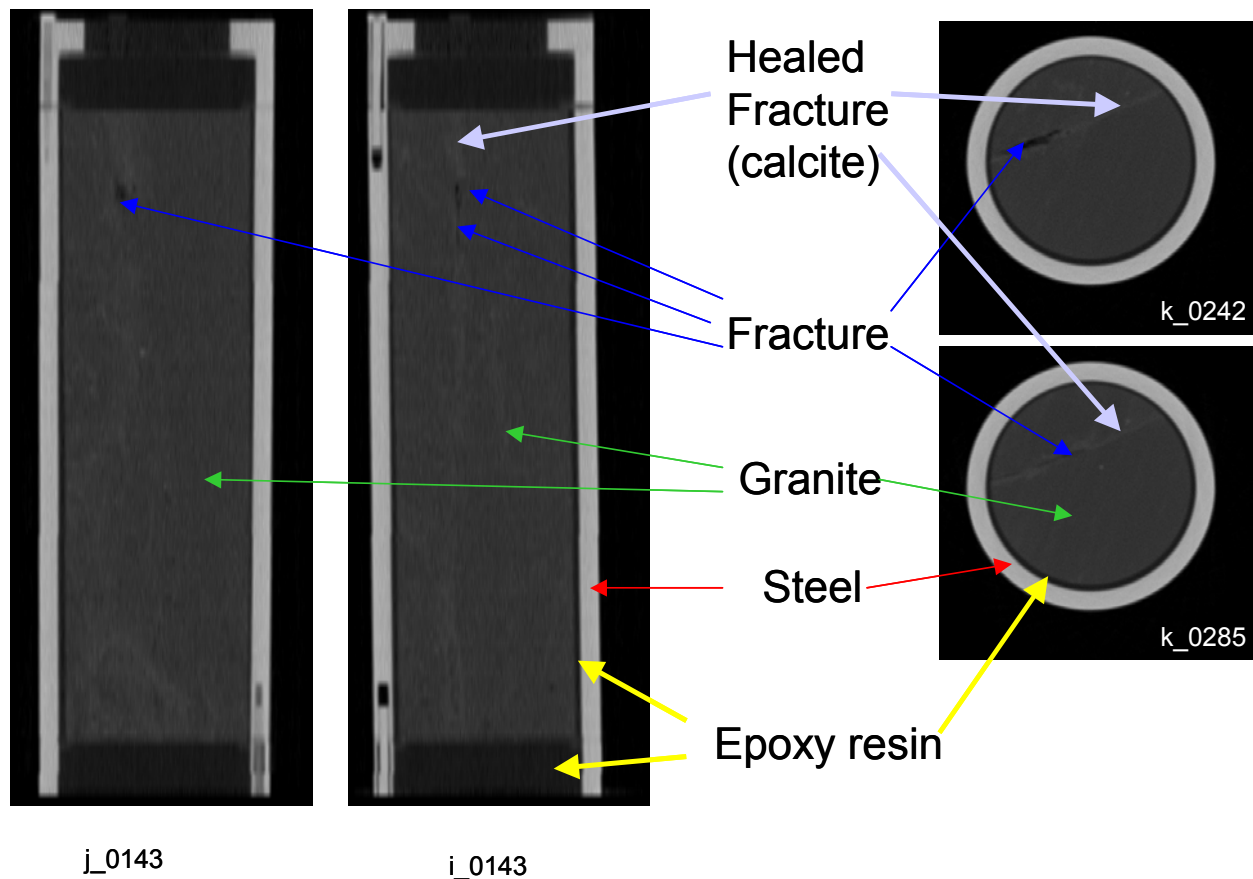


Fig. 5 X-ray computer tomography of core #3  
light-colored: high density  
dark colored: low density

<sup>a</sup> X-ray tomography including graphical representation was performed by Bundesanstalt für Material Forschung in Berlin (BAM)

### 4.3.2 Destructive method

Destructive investigations are performed as follows: The fluorescent epoxy resin was pumped into the fractures after drying the system by injection of isopropanol. The epoxy resin itself had a viscosity, significantly above the value of groundwater<sup>b</sup>. For this reason, especially for core #2 a pressure of about 100 bars was required. After injection of the fluorescent epoxy resin the cores are cut perpendicular to the cylinder axis. This sampling preparation was done with the cores #1 and #2. Resulting slices have a thickness of 3 mm, the thickness of the diamond cutting blade was 0.7 mm. Scanning of the resulting slices shows the geometry, orientation and the properties of the fractures.

Fig. 6 and Fig. 7 show examples of slices of both cores.

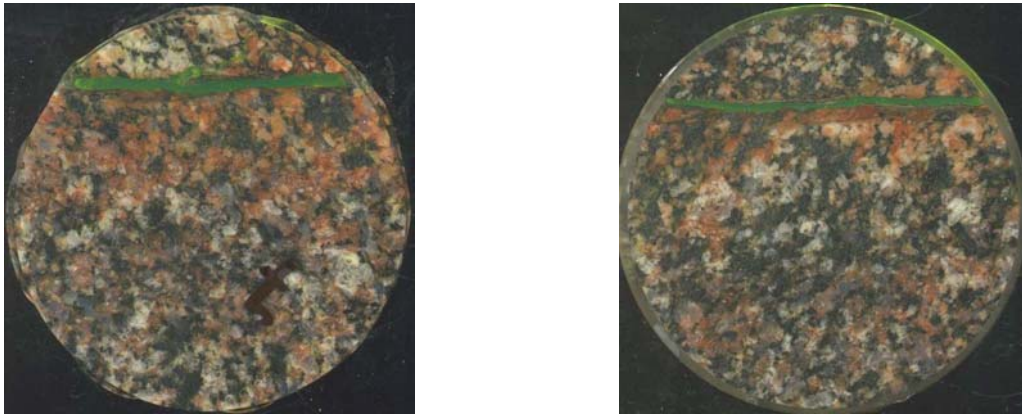


Fig. 6 Scans of slice #7 (left) and #11 (right) of core sample #1  
green colored: fracture filled with fluorescent epoxy resin

Different as in core #1 no flow path could be detected in core #2 by means of scanning for the fluorescent resin. The structures which can be seen in the scans are attributed to a healed fracture system. Volumes of the fluorescent resin are too small to be found by this technique.

---

<sup>b</sup> 4 ml of epoxy resin was mixed with 2 ml of hardener and diluted by 0.5 ml of acetone yielding a viscosity of 30 mPa·s (water at 20°C: 1 mPa·s).

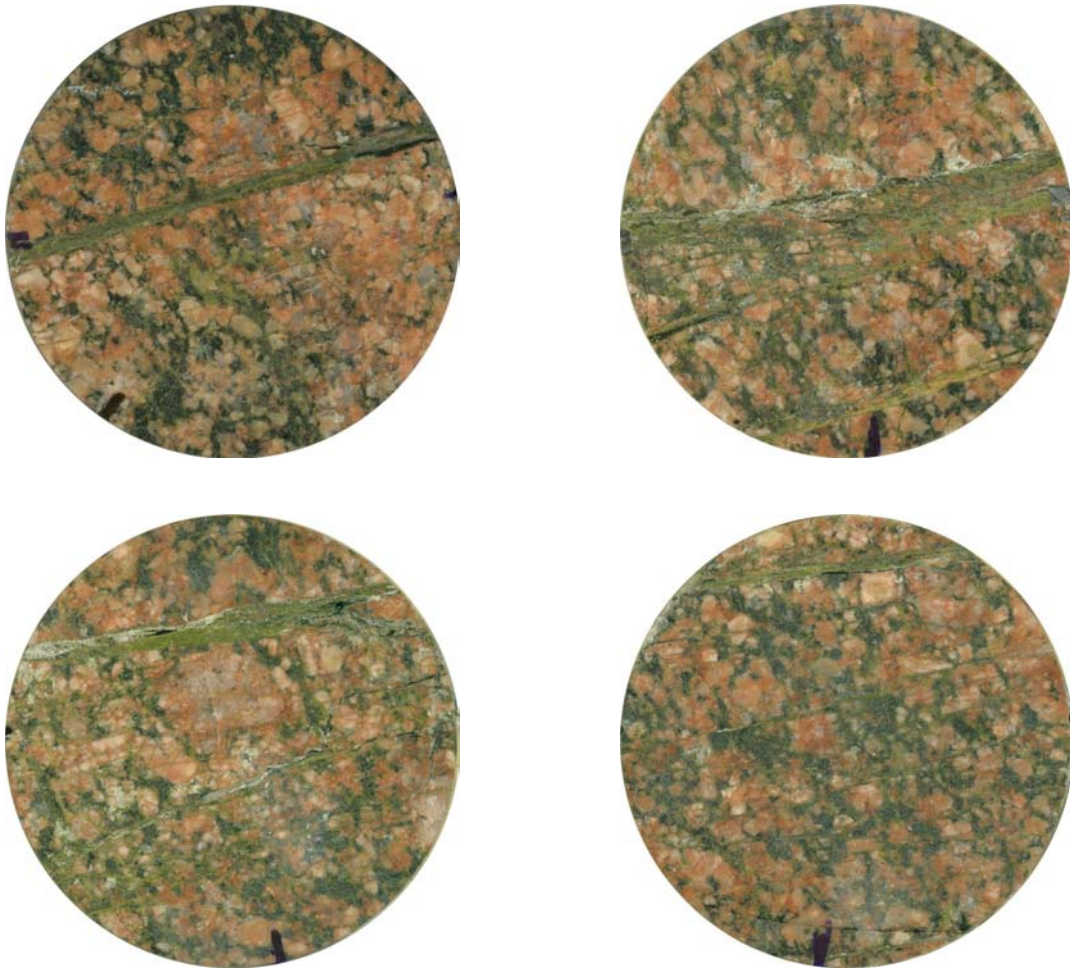


Fig. 7 Scan of slice #1, #10 (top) and #20 and #31 (bottom) of core #2 (used in the first in situ experiment).

In this figure, green colors are attributed to minerals and are not correlated with epoxy resin in open fractures.



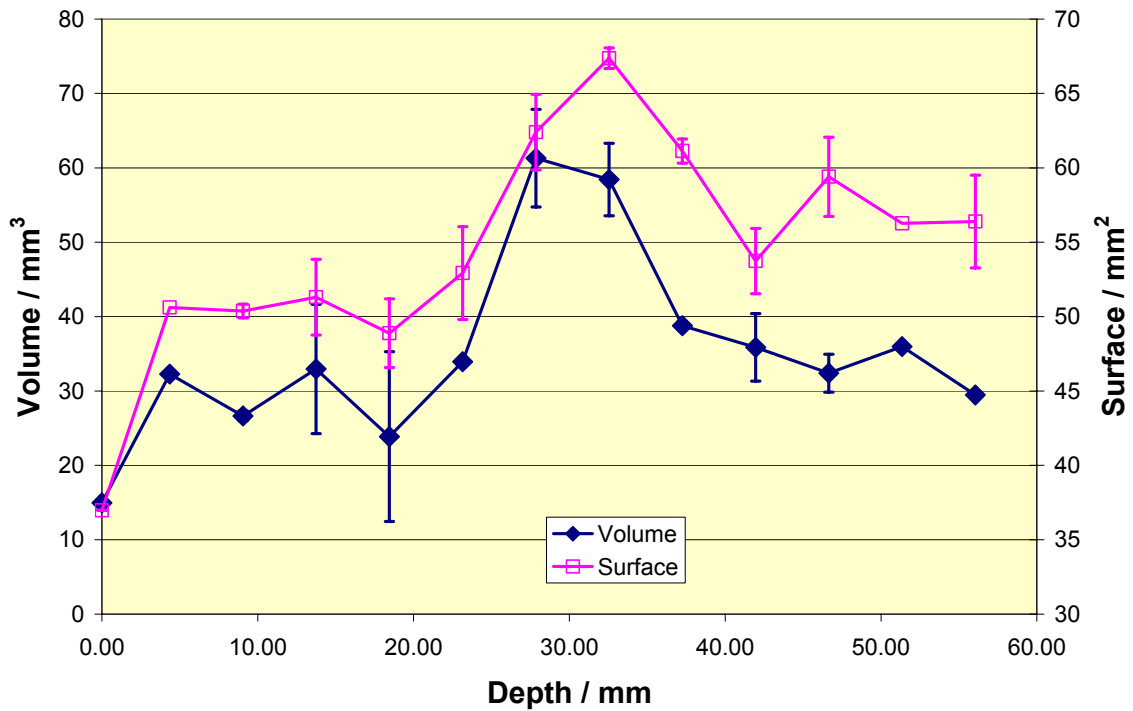


Fig. 8 Distribution of volume and inner surfaces of the fracture along core #1

For core #1 the volume and the inner surfaces of the fracture can be determined from the scans by means of pixel counting. The quantities are given in Tab. III.

Tab. III Evaluation of fracture geometry from slices cut from core #1

Slice Number	Depth / mm	Surface area mm <sup>2</sup>	Volume mm <sup>3</sup>
inlet	0.00	52.83	21.36
1	4.35	72.30	46.11
2	9.05	71.97	38.07
3	13.75	73.30	47.09
4	18.45	69.83	34.09
5	23.15	75.61	48.48
6	27.85	89.14	87.57
7	32.55	96.24	83.47
8	37.25	87.33	55.37
9	41.95	76.76	51.23
10	46.65	84.85	46.27
11	51.35	80.39	51.38
12	56.05	80.56	42.10

Additional information of the flow path can be obtained by 3D visualization of the fracture. For visualization the scans of the slices are used and the fracture (core #1) is discriminated by

selection of the color of the fluorescent resin. Numerically the slices are oriented and by means of the AVS software, the fracture could be visualized.

A three-dimensional image of the fracture in core #1 is shown in Fig. 9.

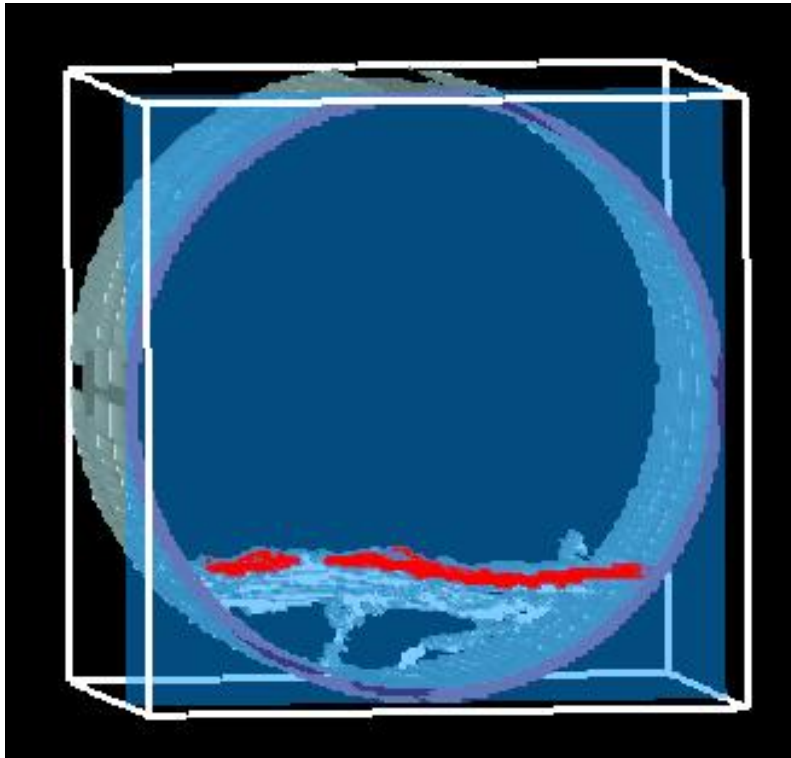


Fig. 9 3-D visualization of the fracture in core #1 by means of AVS software

#### 4.4 Actinides sorbed onto inner surfaces of fractures

Investigations of the distribution of actinides and the sorption behaviour along the flow path can be obtained by different methods. The abraded material gained by cutting the slices was solubilized chemically and the actinide concentration was measured by ICP-MS. The distribution of  $^{237}\text{Np}$  and  $^{243}\text{Am}$  is shown in Fig. 10. Only in a few slices  $^{244}\text{Pu}$  could be detected. Pu concentration is found in the range of the detection limit.

The actinide concentration in the solid material of the slices was analyzed by means of  $\alpha$ -counting and by coupled laser ablation ICP-MS techniques. Laser ablation technique data are not yet available. In addition preliminary measurements of the actinide concentrations have been conducted by micro  $\alpha$ -radiography<sup>c</sup>. Further investigations using this new technique will be performed.

---

<sup>c</sup> Measurements shown in Fig. 11 are performed by a Micro-Imager M40 (Zinsser Analytic, Frankfurt, Germany) having a spatial resolution of 10-15  $\mu\text{m}$ .

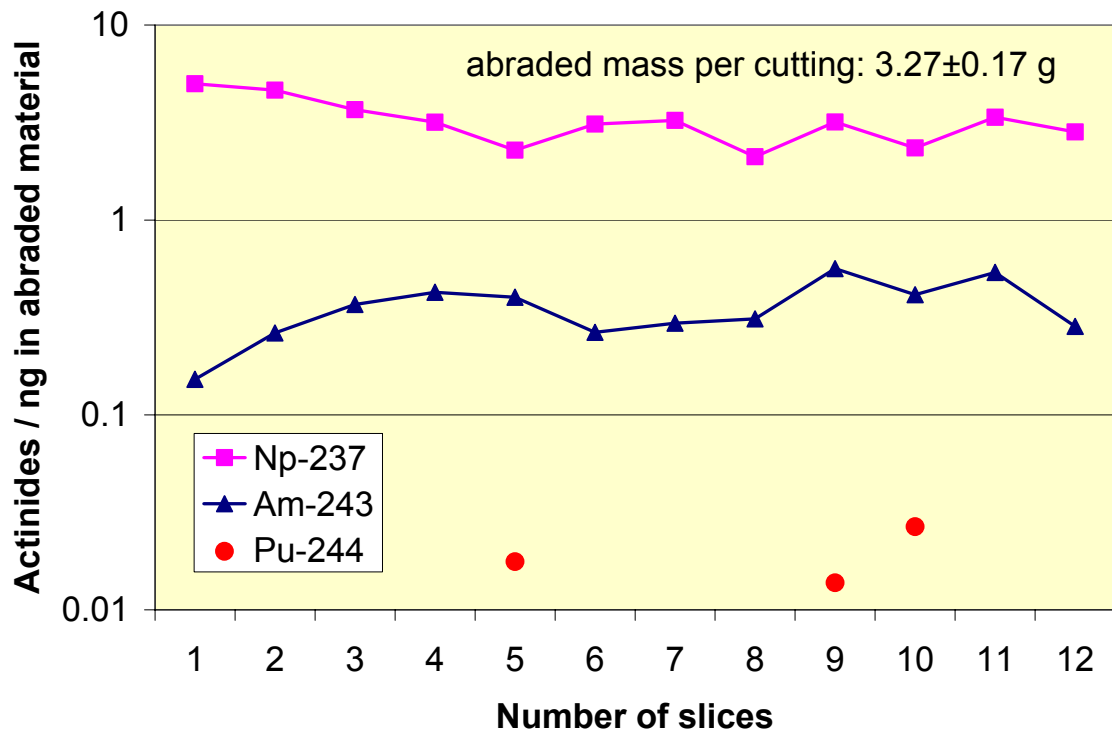


Fig. 10 Distributions of  $^{237}\text{Np}$  and  $^{243}\text{Am}$  along the fracture of core #1 by analysis of the material abraded during the cutting of slices.

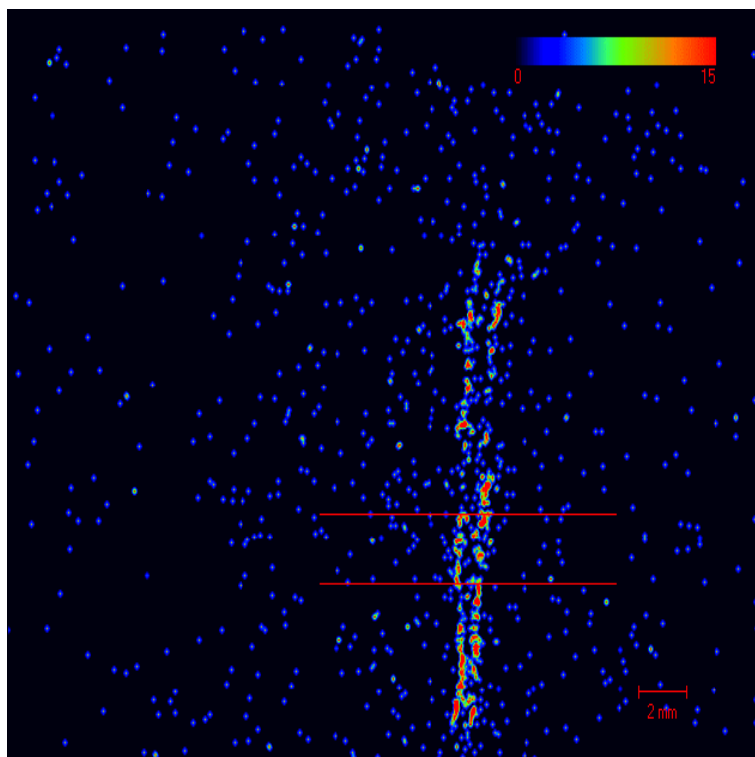


Fig. 11 Investigations of distribution of actinides across a slice of core #1, preliminary results.

In Fig. 11 the distribution of sorbed actinides (mainly Am) on a slice surface is represented by decays of the  $\alpha$ -emitters. The location of actinides can clearly be identified at the surfaces of the fracture. The method applied for these preliminary investigations provides a great potential for characterization of sorbed radionuclides onto mineral phases along the flow path.

## 5 Interpretation of results and discussion

At present, most information is available for core #1. A total of 9 actinide migration experiments are performed using core #1. Interpretation of results for this core is not easy, because a variety of experiments testing the equipment, the injection, influence of flow rates and the detection methodology have been conducted using core #1. For this reason, only tendencies can be derived.

For core #1, the correlation between the actinide concentration determined onto the inner surfaces of the fracture and the geometry of the fracture is investigated. From data shown in Fig. 10 and Fig. 8 the local surface loading density of sorbed actinides is computed and shown in Fig. 12.

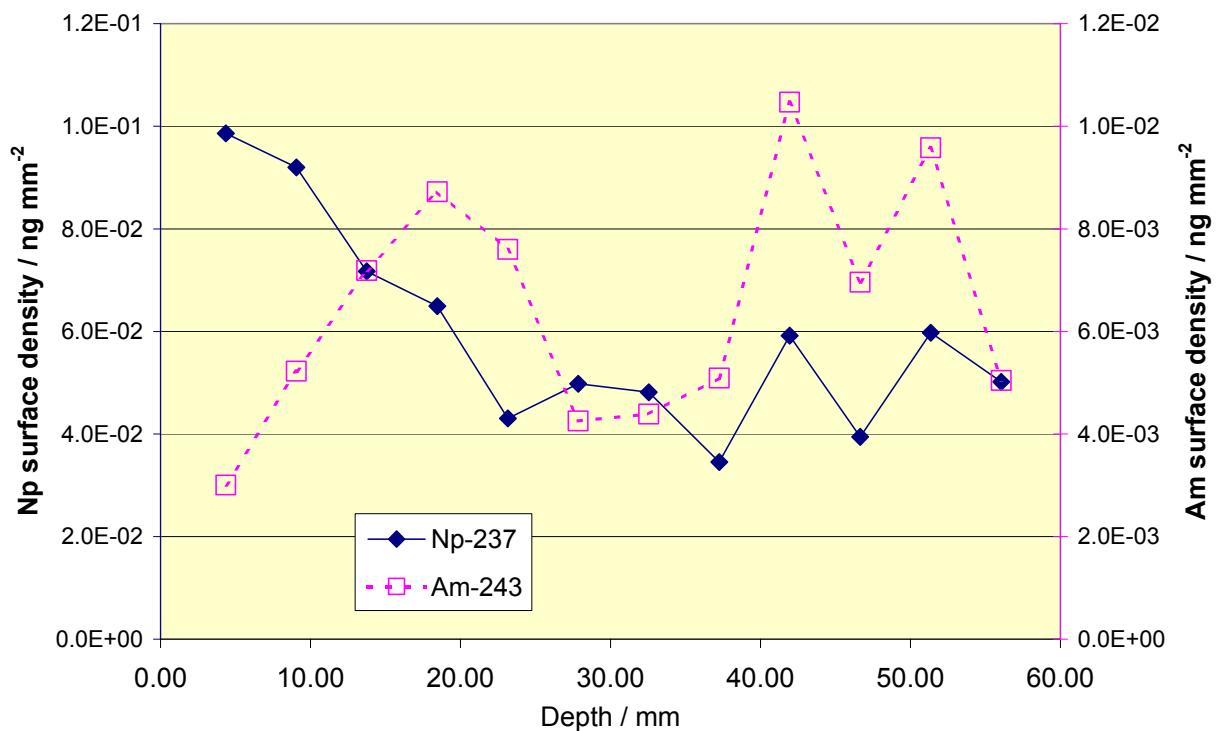


Fig. 12 Locally sorbed actinide surface loading density (Np and Am) determined in core #1

The Np distribution shows a continuous decrease of the surface loading density from the injection to a depth of 23 mm. Measurement at zero depth (injection plane) is not possible, at the moment. At 4.35 mm (slice thickness of 4 mm for core #1 and half of diamond blade having 0.7 mm thickness) from injection, Np surface density is about 0.1 ng/mm<sup>2</sup>. Between 23 mm and 56 mm Np surface density scatters between about 0.06 and 0.04 ng/mm<sup>2</sup>.

Integration of the locally sorbed surface loading density of Np between 4.35 and 23.15 mm result in an total amount of 117 ng Np equivalent to  $0.5 \times 10^{-9}$  mol. 250 ng are computed between 4.35 and 56.0 mm. This amount has to be compared to the totally injected  $^{237}\text{Np}$ . In each of the nine experiments about 50  $\mu\text{l}$  of actinide cocktail was injected, having a Np concentration of  $1 \times 10^{-5}$  mol/l. Arithmetic results that more of one tenth of totally injected  $^{237}\text{Np}$  remains in a depth between 4.35 and 23.15 mm from the injection and more than 20% between 4.35 and 56.0 mm. This finding corroborates well with findings of batch sorption experiments, where it was shown that Np(V) was reduced and precipitated to Np(IV) in the presence of granitic material. It does not contradict measured recovery data, as recoveries between 10 and 40 % are found.

A similar analysis can be done for  $^{243}\text{Am}$ . For Am recovery is below detection limit. This means that almost the total amount of Am injected remains sorbed within the core. In the previous report (Vejmelka 2000), batch sorption data are given. The data varied between 70 and 850 ml/g for material <1 mm grain size and between 10 and 433 ml/g for larger grain sizes. By assuming a certain specific surface area of the material under investigation, the  $R_s$  values can be recomputed to a surface related quantity. However, the question remains what is the relevant specific surface area.

Specific surface areas of the material < 1 mm are measured to be about  $1.1 \text{ m}^2/\text{g}$  using BET  $\text{N}_2$  adsorption analysis. However, this value cannot be compared to the geometric surface determined by the scans of the different slices. The surface areas of the fracture represents a gross geometric feature and not the microscopic surface properties determined by BET. For this reason, the mean surface area of the batch sorption material is computed by a simple geometric approach, assuming a mean diameter of 0.7 mm of each grain and a density of  $2.6 \text{ g/cm}^3$  of the material. Under this assumption the data given in Tab. IV are obtained.

Correlating surface of the fracture with its volume (see Fig. 8) a mean surface to volume ratio of  $1.7 \text{ mm}^2/\text{mm}^3$  is computed. Multiplication of the surface related  $R_s$  value of Tab. IV with the mean surface to fracture volume ratio results in values between 34 and 442 for the fine grained material and between 5.1 and 221 for the gross material. These ratios are dimensionless, representing the retardation of the actinide (Am) against an inert tracer.

Tab. IV Mass and surface related  $R_s$  values of Am onto granitic material

	$R_s$ (mass related)	$R_s$ (surface related)	$R_s$ (mass related)	$R_s$ (surface related)
Dimension	ml/g	ml/mm <sup>2</sup>	ml/g	ml/mm <sup>2</sup>
	$R_s$	$R_s$	$R_s$	$R_s$
Time / d	fraction < 1mm	fraction <1mm	fraction > 1mm	fraction >1mm
0	70.12	0.02	9.97	0.003
2	79.59	0.02	36.25	0.01
8	278.40	0.08	66.11	0.02
18	315.62	0.10		
28	353.65	0.11	143.19	0.04
63	850.37	0.26	433.07	0.13

The range of retardation values determined by batch experiments can be compared with findings of the migration experiments. The Am peak determined at 18.45 mm from the injection is correlated to last experiment performed at this core.

Taking data from Tab. II, migration time of the injected pulse can be computed. In the two last experiments very low flow rates were applied. Total duration of the experiment lasted for 40000 minutes with a totally eluted volume of 40 ml water and a mean velocity of the groundwater of 0.02 mm/min. As Fig. 13 shows, migration of Am reached 18.45 mm within 40000 min. The ratio of the migration time of water to the migration time of Am results in a retardation factor for Am which amounts to 43. This value is in the range of  $R_s$  values reported above.

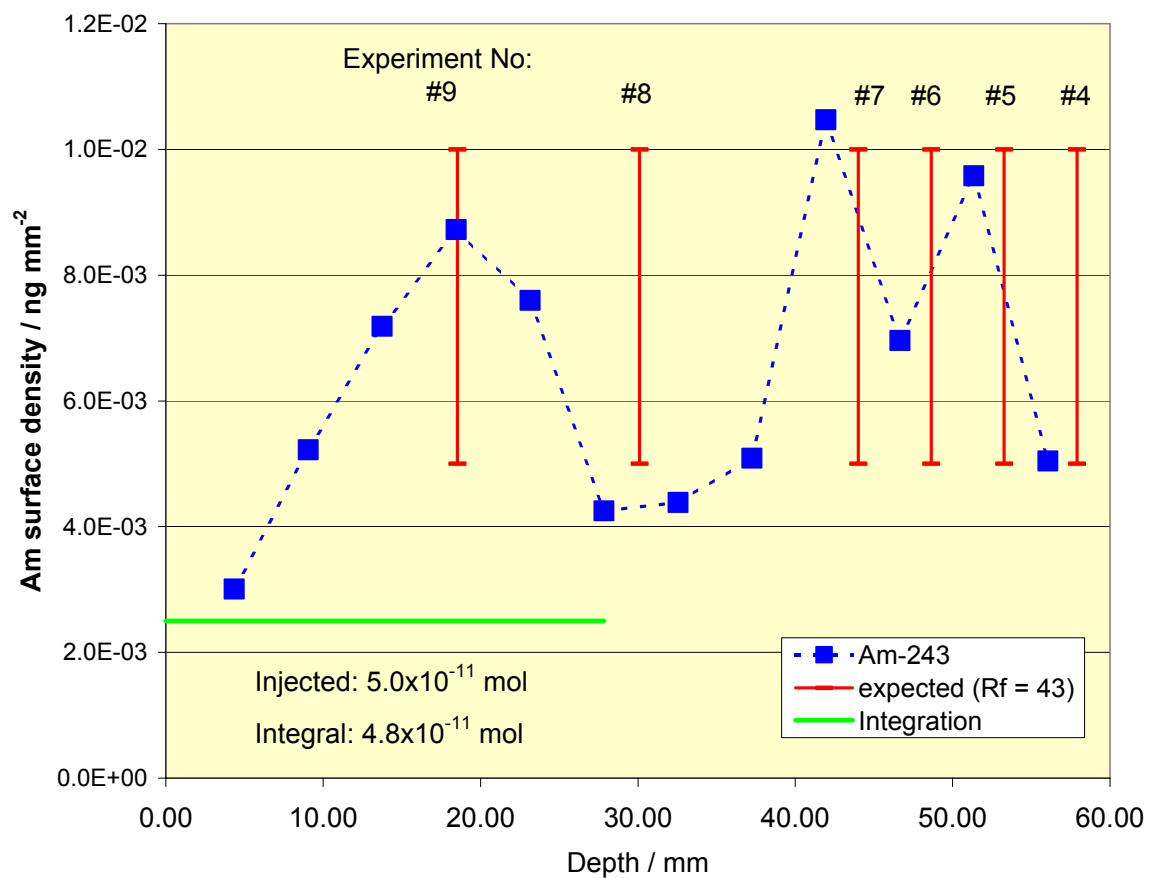


Fig. 13 Locally sorbed <sup>243</sup>Am distribution in core #1

Recursively, the expected Am peaks can also be computed for the different experiments with core #1. Only in the last 2 experiments, the low flow rates are used. The vertical lines shown in Fig. 13 represent the expected maximum concentrations for the different experiments characterized in Tab. II. These experiments however, are not performed consecutively, and a certain time dependence of sorption was observed for Am, too (see Tab. IV). Therefore the interpretation of the fluctuations of the sorbed <sup>243</sup>Am concentration is speculative to some extent.

## 5.1 Hydraulic properties

For interpretation of the breakthrough of the actinides, the hydraulic properties of the fractured cores are required. Hydraulic properties, such as effective porosity, dispersion coefficient, breakthrough time can be determined by evaluating measured breakthrough curves of non sorbing tracer like HTO. Breakthrough curves for HTO are shown in ref. (Vejmelka 2000). The zero<sup>th</sup>, first and second order momentums of the time dependend breakthrough curves are computed. A corresponding evaluation is given by (Appelo 1994).

The breakthrough time is computed as ratio of the first by the zero<sup>th</sup> momentum

$$t_0 = \frac{\sum t_i \cdot c_i}{\sum c_i}$$

Dividing the core length  $l$  by the breakthrough time  $t_0$  results in the pore water velocity  $v_0$ .

$$v_0 = \frac{l}{t_0}$$

The variance of the breakthrough curve  $\sigma_t^2$  is given by the ratio of the second by the zero<sup>th</sup> momentum related to the breakthrough time  $t_0$ .

$$\sigma_t^2 = \frac{\sum t_i^2 \cdot c_i}{\sum c_i} - t_0^2$$

From time related  $\sigma_t^2$  the longitudinal dispersion coefficient  $\sigma_x^2$  is obtained by

$$\sigma_x^2 = \frac{\sigma_t^2}{t_0^2} \cdot l^2$$

The dispersion coefficient is calculated by

$$D = \frac{\sigma_x^2}{2 \cdot t_0}$$

and the dispersion length  $\alpha$  by

$$\alpha = \frac{D}{v_0}$$

For modeling, the Peclet number  $Pe$  is required, which is given by the definition

$$Pe = \frac{v_0 \cdot l}{D}$$

For some HTO breakthrough curves these data are evaluated. Pulse injection of about 50  $\mu$ l of HTO solution was applied. Background subtraction is performed by defining a minimum HTO concentration of the breakthrough peak. The results are shown in the following table Tab. V.

Tab. V Hydraulic properties of core #2

Test		C2HTO2	C2HTO3	C2HTO6	C2HTO4a
<b>Flow rate</b>		0.05 ml/min	0.05 ml/min	0.05 ml/min	0.001 ml/min
<b>l</b>	m	0.15	0.15	0.15	0.15
<b>t<sub>0</sub></b>	s	2571	2335	2445	179139
<b>v<sub>0</sub></b>	m/s	5.83E-05	6.42E-05	6.14E-05	8.37E-07
<b>σ<sub>t</sub><sup>2</sup></b>	-	1.040	1.044	1.048	1.063
<b>D</b>	m <sup>2</sup> /s	4.55E-06	5.03E-06	4.82E-06	6.68E-08
<b>α</b>	m	7.80E-02	7.83E-02	7.86E-02	7.97E-02
<b>Pore Volume (momentum)</b>	ml	2.1	1.9	2.0	3.0
<b>Porosity</b>	%	0.71	0.65	0.68	1.00
<b>Peclet Number</b>	-	1.92	1.92	1.91	1.88

Dividing the Darcy velocity determined from the flow rate by the pore water velocity  $v_0$  the effective porosity of the core is obtained. However, this assumption, is ambiguous because it is defined for porous media, only. But, as one can see from the cuts through core #2 in Fig. 7, a well-defined fracture is not present.

## 5.2 Actinide speciation

The laboratory experiments are performed in a glove box at a 99%Ar, 1%CO<sub>2</sub> atmosphere. At Äspö HRL, under the prevailing condition in the CHEMLAB drill hole, the CO<sub>2</sub> partial-pressure may be different from the conditions in the glovebox. Accordingly, the actinides speciation may vary under the different conditions. Depending on the speciation, the sorption/migration behavior of these elements may be different. For this reason the speciation of the actinides in concentrations used in the actinide cocktail is computed using the Geochemist's Workbench code (GWB 1999). The following figures show the relevant actinide species depending on the CO<sub>2</sub> partial pressure. Composition of groundwater in this drill hole was measured by SKB (May 10,1999), the data reported by Anna Säfvestad are given in Tab. VI.

HCO<sub>3</sub><sup>-</sup> concentration and pH can be applied to calculate the pCO<sub>2</sub> for the groundwater according

$$[\text{HCO}_3^-] = 10^{-7.8} \cdot p_{\text{CO}_2} / [\text{H}^+]$$

Using the data of Tab. VI results in  $p_{\text{CO}_2} = 2.5 \times 10^{-3}$  bar or  $\log p_{\text{CO}_2} = -2.6$ .



Tab. VI Composition of groundwater from CHEMLAB-2 drill hole

Element	CHEMLAB-2 [molar]
Na	8.96E-02
K	2.05E-04
Ca	4.07E-02
Mg	2.43E-03
HCO <sub>3</sub>	1.00E-03
Cl	1.75E-01
SO <sub>4</sub>	4.92E-03
Si	2.21E-04
Fe	2.67E-06
Mn	8.37E-06
Li	1.54E-04
Sr	2.91E-04
pH	7.4

Laboratory experiments are performed at  $p_{\text{CO}_2}$  of 0.01 bar which is by a factor of 4 above  $p_{\text{CO}_2}$  at the CHEMLAB-2 site. Fig. 14 shows clearly that at  $\text{CO}_2$  partial pressure of laboratory and CHEMLAB conditions, the dominating dissolved Pu(IV) species is  $\text{Pu}(\text{OH})_3\text{CO}_3^-$ , only at significantly higher  $\text{CO}_2$  partial pressures  $\text{Pu}(\text{OH})_2(\text{CO}_3)_2^{2-}$  would dominate.

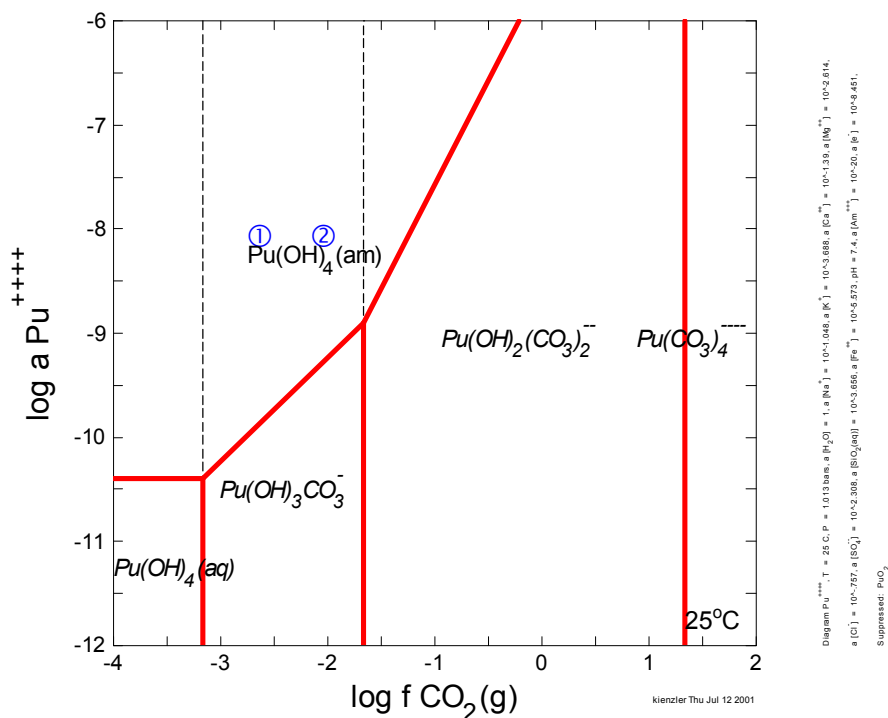


Fig. 14 Speciation of plutonium in Äspö groundwater in dependence on the  $\text{CO}_2$  partial pressure.  
①: CHEMLAB-2 conditions, ②: laboratory conditions

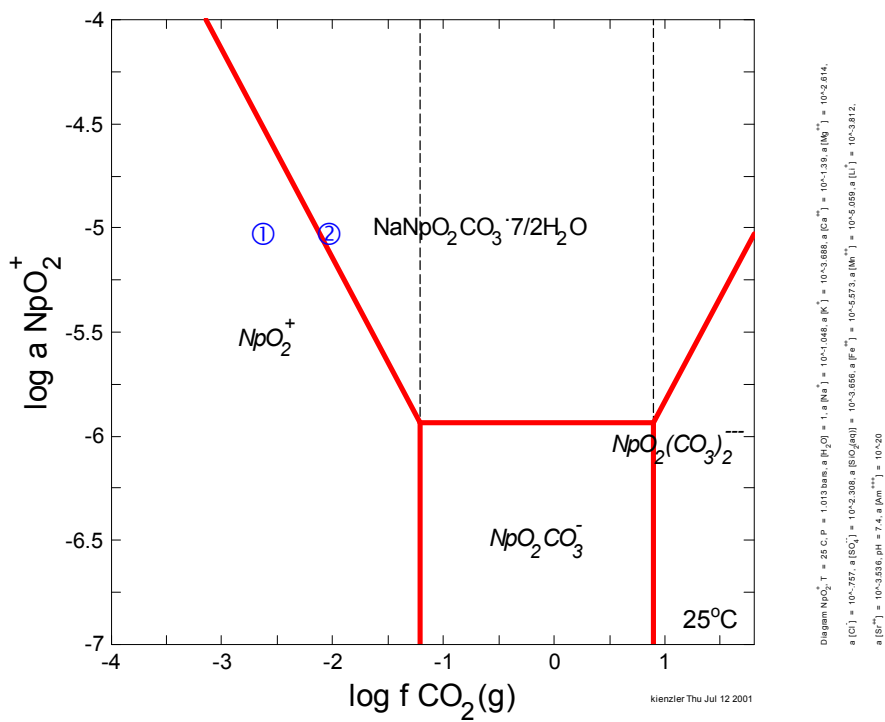


Fig. 15 Speciation of neptunium in Äspö groundwater in dependence on the CO<sub>2</sub> partial pressure.

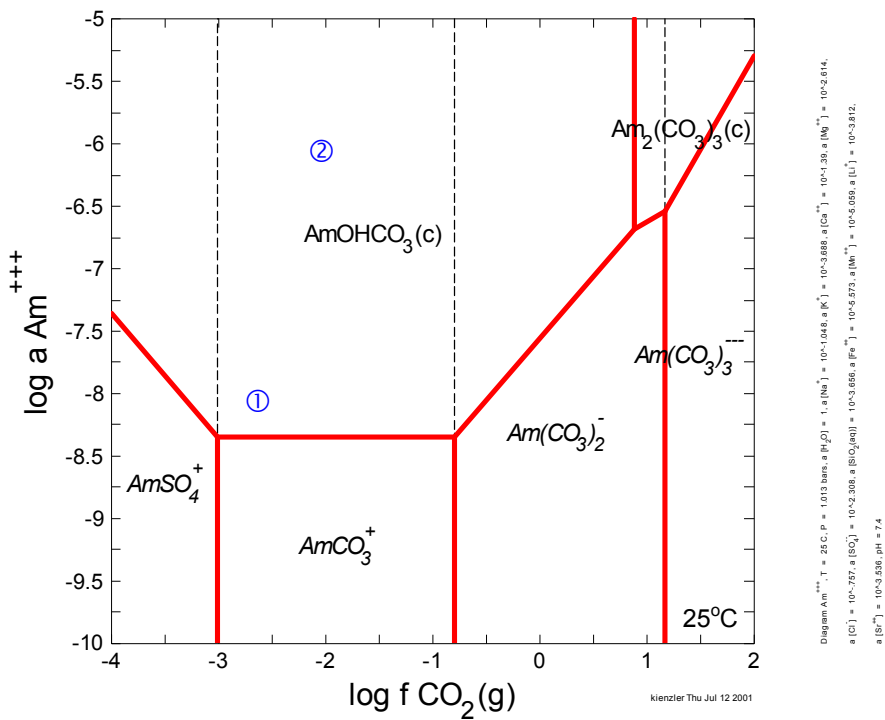


Fig. 16 Speciation of americium in Äspö groundwater in dependence on the CO<sub>2</sub> partial pressure.

Am(III) exists as mono- carbonato species under the prevailing conditions of laboratory and CHEMLAB-2. For Np(V) under laboratory and CHEMLAB-2 conditions only  $\text{NpO}_2^+$  species are expected. This assumption was verified by UV-VIS-NIR spectroscopy

Solution sampled at the peak of the breakthrough of the CHEMLAB-2 experiment was tightly closed and transferred to INE. UV-VIS-NIR spectroscopy was performed with a Cary 5 spectrophotometer (VARIAN) in a 1 cm quartz cuvette. The solution eluted in the Äspö experiment was poured in a cuvette in glove boxes under an Argon / 1 %  $\text{CO}_2$  atmosphere. The absorption spectra were taken in the wavelength range 920 to 1040 nm. The spectrum shows only one absorption band with a maximum at 980.4 nm corresponding to a free uncomplexed neptunyl ion ( $\text{NpO}_2^+$ ). By using the absorption coefficient of  $395 \text{ L mol}^{-1} \text{ cm}^{-1}$  a concentration of  $\text{NpO}_2^+$  of  $9 \cdot 10^{-6} \text{ mol/L}$  was estimated which corresponds to the total neptunium concentration measured by liquid scintillation counting. No Np(V) carbonate complexes and no Np(IV)-species could be detected by absorption spectroscopy.

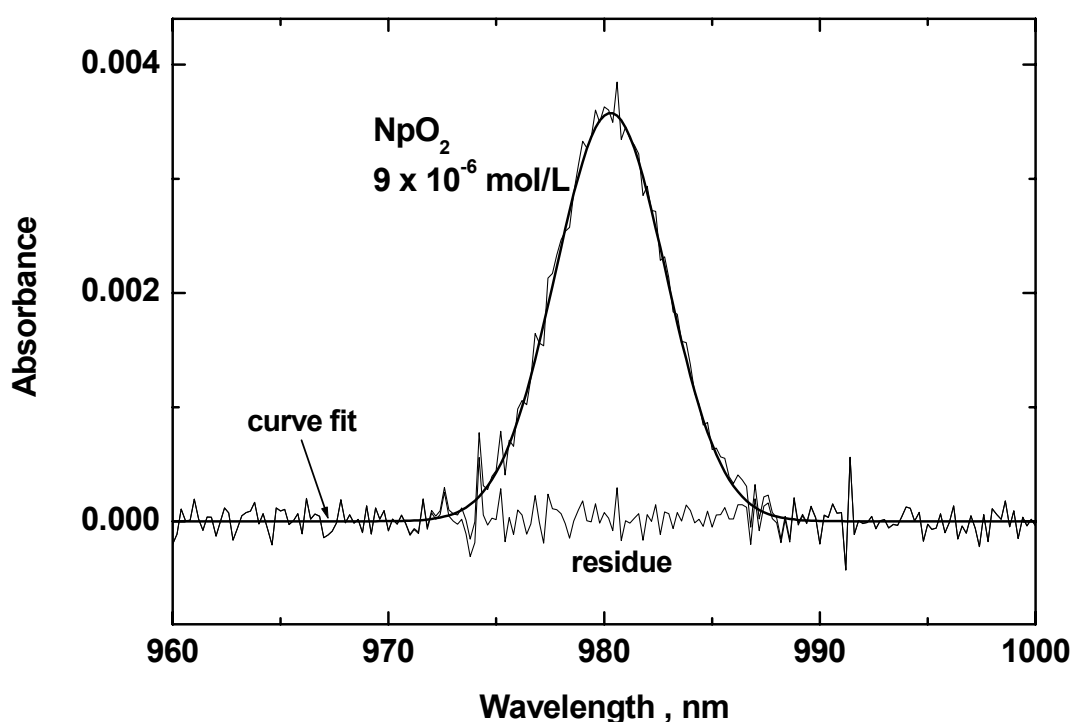


Fig. 17 UV-VIS-NIR spectroscopy of eluted solution sampled in the breakthrough peak of the CHEMLAB experiment (core #2) at Äspö HRL.

### 5.3 Modeling actinide breakthrough and recovery

Breakthrough and recovery of HTO and the actinides in core #2 experiment at Äspö are compared to computed results. Computation is performed by means of the one-dimensional TRANS\_EQL code (Kienzler 1995). Input data are taken from Tab. V. Fig. 7 shows that an

open fracture similar to core #1 is not available. For this reason, the core #2 is modeled using a porous medium approach.

The comparison between computations and experiment is shown in Fig. 18. Experimental volume fractions given in the figure are corrected with respect to evaporation of water during the sampling period<sup>d</sup>. It is obvious, that computed breakthrough does not reflect the observations satisfactorily.

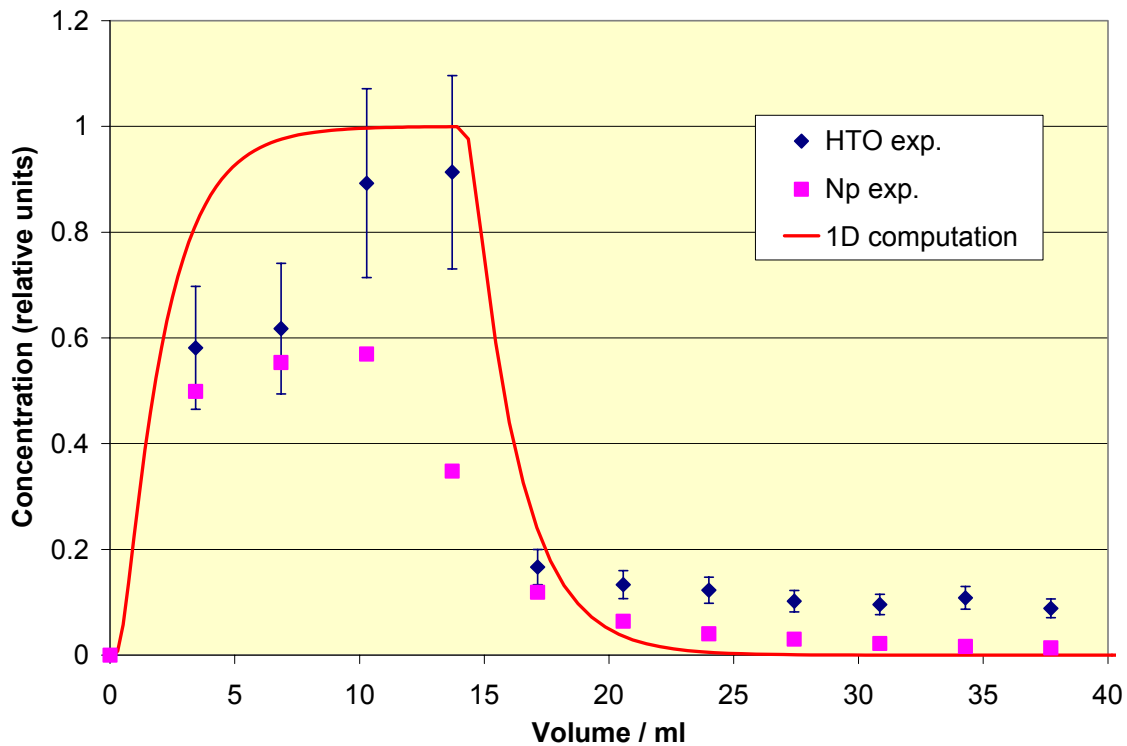


Fig. 18 Comparison between computed and experimental breakthrough for the CHEMLAB experiment (core #2, scale shifted with respect to dead volume)

Reasons of the discrepancy between the HTO curve and computations for an inert tracer are certainly attributed to very complex flow pattern in the partly fractured core #2. The complicated flow path cannot be described by the model. The model applied works well, if the system can be averaged by a porous media. Application of a more sophisticated fracture flow model is constrained by the lack of information about the geometry of the flow path. This information will be determined by measurement of the concentrations of sorbed actinides by means of laser ablation techniques or by micro  $\alpha$ -radiography. These measurements will result in a non uniform distribution of sorbed actinides which may follow the distribution of pores and their interconnections. These data are not yet available.

Breakthrough of Np follows in the tendency both the measured HTO curve as well as the computed breakthrough of an inert tracer. The comparison shows that Np migrates unretardedly. Integration of the Np breakthrough results in a recovery of about 40% of the injected amount. In contrast, 100% elution of the tracer is computed in the example shown above. The observed behavior cannot be described by a simple sorption model. Precipitation

<sup>d</sup> For the applied flow rate, a loss of water of 30% per sample was measured in the Äspö glove box.

processes have to be taken into account, as shown in batch sorption experiments. In the case of Np(V) precipitation is expected only, if a reduction to Np(IV) occurs.

The flow path and its corresponding surface characteristics as well as its specific surface sizes are not known. As these data are required in a reliable model, unfortunately fitting of these parameters would have to be performed.

## 5.4 Matrix diffusion?

Many conceptual models describing tracer migration in complex granitic systems take matrix diffusion processes into account. Theoretical considerations show that the response function, such as the elution curve of a pulse injection should follow the following relation (Hadermann1994, Barten 1996).

$$f = const. \cdot t^{-\frac{3}{2}}$$

This function is shown in Fig. 19. The relation is valid in the case of "unlimited" matrix diffusion which means that the system is not restrained in geometry. Core #2, however, is enclosed in an autoclave. For this reason, it is obvious that deviations between measured and computed response functions are expected.

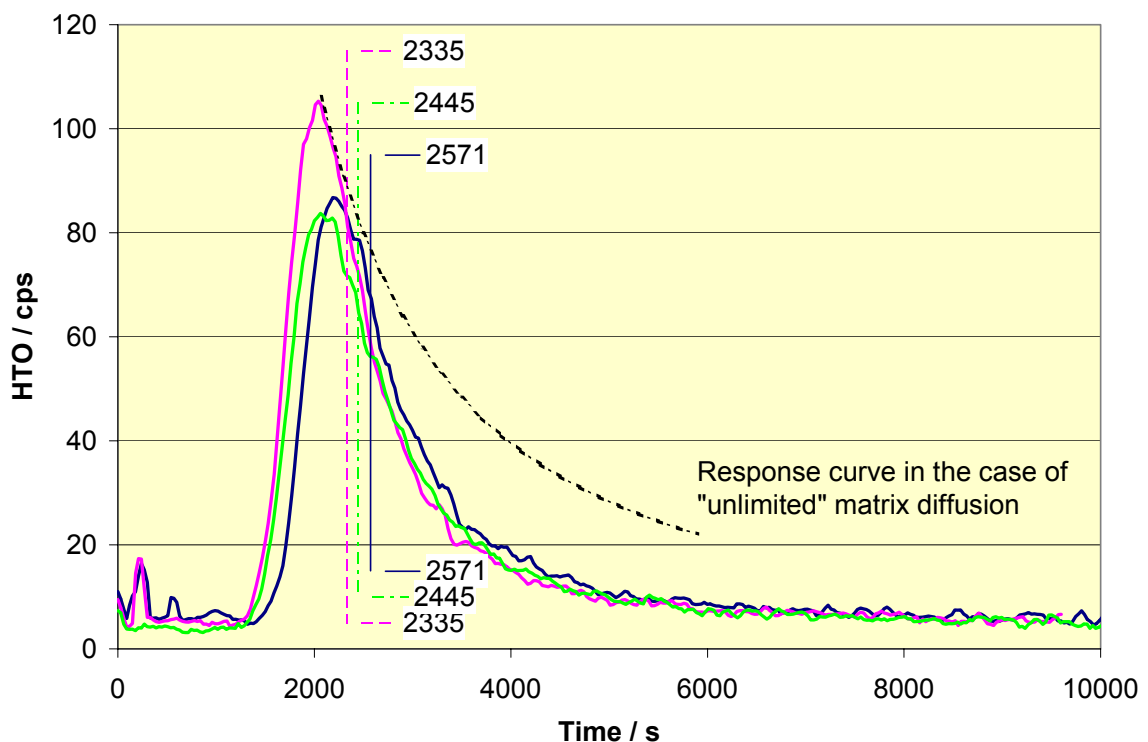


Fig. 19 Breakthrough curves obtained in core #2 for HTO pulse injection.  
 Vertical lines: computed breakthrough time  $t_0$   
 Dotted line: Theoretical response function in the case of matrix diffusion

## 6 Summary and conclusions

Following conclusions can be drawn from the results of the actinide migration experiments:

- The design of the drill cores enclosed in stainless steel autoclaves, the tubings made of PEEK material, and the tubing connectors fit excellently with the demands for laboratory as well as for the in situ experiments.
- Sampling by fraction collectors and drop counting is adequate for the experiments. However, an evaporation rate of droplets has to be taken into account and corrected by calibration. Further experiments will apply closed vials using an appropriate fraction collector.
- The migration experiments performed in laboratory and in the CHEMLAB probe complement on another. Batch experiments are essential to get information for the layout of an experimental schema. CO<sub>2</sub> partial pressure adjusted in laboratory results in the same actinide speciation as expected under in situ conditions.
- Determination of hydraulic properties by means of inert HTO tracer and application of different flow rates is an effective procedure, resulting in data to be required for modeling.
- Destructive and non-destructive analyses of flow paths have to be applied in order to obtain most complete information. In the case of open fractures (core #1), application of fluorescent epoxy resin, cutting and scanning of slices quantifies the volume and the surface of the fractures
- Abraded material gained by cutting the cores can be dissolved and actinide concentrations be measured by ICP-MS. Even in the case of pulse injection of actinides, it was possible to determine the sorbed actinides in the abraded material.
- The cores investigated up to now show different specific pattern of the flow path. Core #1 had a flow path attributed to a single fracture, whereas core #2, #3, and #4 have only partly open fractures. Especially in some parts of the cores (#2, #3, and #4) the ground water flow penetrates small sized flow paths which cannot be detected and evaluated by used methods. As a consequence, for future experiments single fractured cores are under preparation.
- Experiments using cores #2 and #4 resulted in breakthrough of Np(V) only. The recovery was in any case  $\leq 40\%$ . Recovery of Am(III) and Pu(IV) as well as of Np(IV) was not detected.
- The model applied is not well suited for the complex flow paths and the complicated sorption processes. Application of more complex models require data on the geometry of the flow path which are not yet available. Matrix diffusion processes seem not to be relevant for core #2.
- Further analytical methods, such as laser ablation techniques and micro  $\alpha$ -radiography have to be applied, in order to get more complete information about the longitudinal and transversal distribution of sorbed actinides.
- Flow rates used in the experiments are high in comparison to natural groundwater velocity. Therefore further experiments will be performed at lower flow rates, however, the rates are constrained by the experimental setup.

## 7 References

- (Appelo 1994) Appelo, C.A.J., D. Postma;  
Geochemistry, groundwater and pollution. A.A. Balkema, Rotterdam, ISBN 905410106,  
1994.
- (Barten 1996), Barten, W.;;  
Linear response concept combining advection and limited rock matrix diffusion in a fracture  
network transport model. Water Resources Research 32, 3285-3296, 1996.
- (Backblom 1991) Backblom, G.;;  
The Aspo Hard Rock Laboratory - a step towards the Swedish final repository for high-level  
radioactive waste. Tunnelling and Underground Space Technology 4(4) p. 463-467, 1991.
- (GWB 1999) Bethke, C.M.;;  
The Geochemist's Workbench, Version 3. University of Illinois, USA, 1999.
- (Hadermann 1996) Hadermann, J.;;  
The Grimsel migration experiment: Integrating field experiments, laboratory investigations  
and modeling. J. Contam. Hydrol. 21, 87-100, 1996.
- (Jansson 1997) Mats Jansson, Trygve E. Erikson;  
CHEMLAB-In-Situ Diffusion Experiments Using Radioactive Tracers, Migration 97.
- (Kienzler 1995) Kienzler, B.;;  
A coupled migration/speciation code - demonstrated by modeling the migration of americium  
in a column. Proc.of the Internat. Conf. on Mathematics and Computations, Reactor Physics,  
and Environmental Analyses, Portland, Oreg., April 30 - May 4, 1995, LaGrange Park, Ill.:  
ANS, 1995 S.421-30.
- (Vejmelka 2000) Vejmélka, P., Th. Fanghänel, B. Kienzler, E. Korthaus, J. Römer,  
W. Schuessler, R. Artinger;  
Sorption and Migration of Radionuclides in Granite (HRL ÄSPÖ, Sweden), FZKA 6488, 2000.